African Journal of Biotechnology Vol. 10(12), pp. 2340-2352, 21 March, 2011
Available online at http://www.academicjournals.org/AJB
DOI: 10.5897/AJB09.974
ISSN 1684–5315 © 2011 Academic Journals

Full Length Research Paper

Metabolic flux distribution and mathematical models for dynamic simulation of carbon metabolism in *Escherichia coli*

Md. Aminul Hoque[1,4,5,*], Kotb Attia[2], Omar Alattas[3] and Amir Feisal Merican[1]

[1]Centre of Research in Computational Sciences and Informaticsin Biology, Biodiversity, Environment, Agriculture and Healthcare (CRYSTAL), Institute of Biological Sciences, Faculty of Science, University of Malaya, Kuala Lumpur-50603, Malaysia.
[2]Graduate School of Science and Technology, Niigata University, Ikarashi-2, Niigata, Japan.
[3]Centre of Excellence in Biotechnology Research, King Saud University, Riyadh 11451, Kingdom of Saudi Arabia.
[4]Graduate School of Medicine, Niigata University, Asahimachi 1-754, Niigata, Japan.
[5]Department of Statistics, Rashahi University, Rajshahi-6205, Bangladesh.

Accepted 14 September, 2009

A simple model was build for the metabolic flux determination based on published articles. A method for metabolic flux determination by carbon labeling experiments was described and developed here in the first part of this study that allows mathematical description relating the measured quantities and the intracellular fluxes. The described method was used to investigate the central carbon metabolism of *Escherichia coli.* In the second part of this study, computer simulation was made to study the dynamics of the intracellular metabolite concentrations in *E. coli* in particular for the glycolysis and pentose-phosphate pathway based on the kinetic rate equations. The model successfully simulates the main features of the time course without alteration of the experimentally determined parameters. After simulation starts, the intracellular concentrations of ATP, PEP, PYR, G6P, F6P, NAD and 3PG decreased while FDP, 6PG, S7P, E4P AMP, GAP, ADP, NADH and NADPH increased for wild *E. coli*. These simulation results were also partly verified by experimental results.

Key words: Metabolic flux, metabolite concentration, computer simulation, optimization technique, parameters.

INTRODUCTION

Conventional metabolic flux analysis has been made based on the measured extracellular flux data and mass conservation law for key intracellular metabolites (Yang et al., 2002; Vallino and Stepphanopoulos, 1993; Theobald et al., 1997; Hua et al., 1998). Due to the insufficient information from metabolite balancing to determine intracellular fluxes, some of the metabolic fluxes such as cyclic pathway, parallel pathway cannot be defined without imposing more assumptions on enzyme activities or energy yields. By the introduction of labeling experiments, it can overcome this problem (Noronha et al., 2000; Park et al., 1997; Sonntag et al., 1995; Wierchert et al., 1997) and these labeling measurement data provide additional and independent constraints on the intracellular fluxes, which enables a more refined analysis of metabolic fluxes in the complex metabolic network.

Microbial growth depends on the biosynthesis of cellular macromolecules (proteins, lipids, amino acids, RNA and DNA), which require NADPH as a redox-equivalent. In *Escherichia coli* NADPH is mainly formed from the pentose phosphate pathway and TCA pathway (Hoque et al., 2005; Lagunas and Gancedo, 1973; Thomas et al., 1991; Sarkar et al., 2008; Nogae and Johnson, 1990). Also a set of precursors for the synthesis of amino acids, cometabolites and nucleotides is provided by these main pathways (Figure 2). One of the recent most challenging and demanding research areas of metabolic engineering is to investigate the dynamics of

*Corresponding author. E-mail: mdaminulh@gmail.com. Phone: +81-25-227-0294 (Office.), Fax: +81-25-227-0850 (Office).

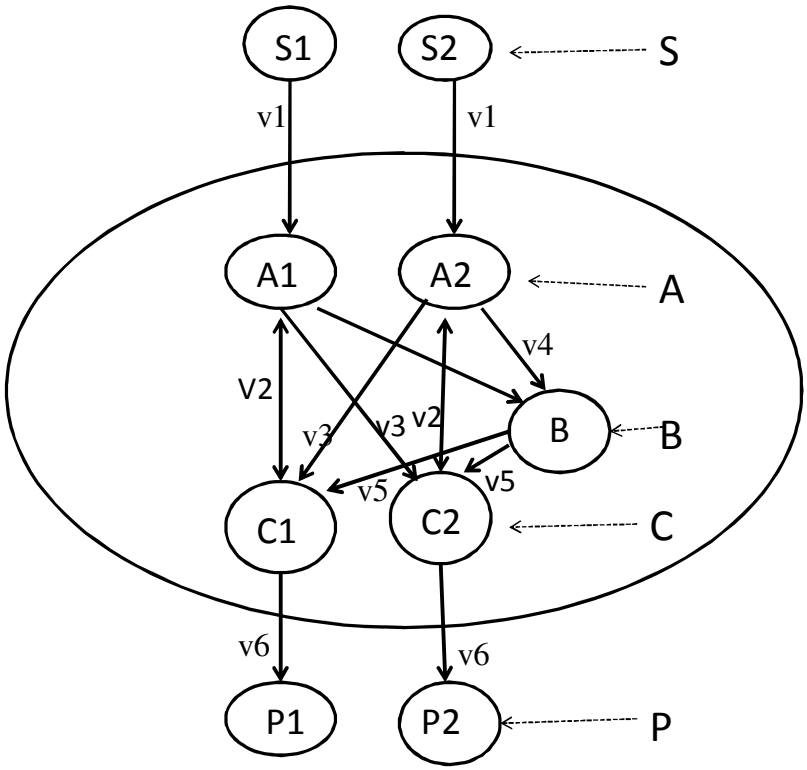

Figure 1. A simple model of comparing two metabolic networks

metabolism and to estimate the control coefficients by using mathematical models. The model development for simulation is useful in that the model may be less expensive in terms of time, more easily studied and more easily controlled than the original (Greco, 1986). In the present study, dynamic simulations based on Chassagnole et al. (2002) and Rizzi et al. (1997) were performed and verified by published experimental results.We also considered a simple model for flux determination to get some idea on how to compute metabolic flux distributions based on measured isotopomer distributions.

MATERIALS AND METHODS

There exist various theories arisen recently to explain various biological phenomena, such as allometrical method to solve various basic problems in biology (He, 2008). Zhou et al. (2009) suggested a simple method for carbon absorption using allometric scaling. These methods sometimes give good result but to meet our goal of the present study we use Yang et al. (2002) method.

A simple model for metabolic flux determination based on isotopomer measurements

Consider a simple metabolic network as shown in Figure 1, where S represents an input (extracellular) metabolite with known isotopomer distribution, A, B and C the intracellular metabolites (intermediates) and P the output metabolite. For simplicity, we assume that B has one carbon atom, and the others have two carbon atoms. In Figure 1, V1 is the measurable input flux, V6 is the output flux and the remaining V2, V3, V4 and V5 are the intracellular fluxes. V2 and V3 keep the metabolite together with different fates of carbon atoms. V2 is the bidirectional flux while the others are unidirectional fluxes. The mass balances for the intracellular metabolites yield:

$$\begin{aligned} &\text{A:} \quad \vec{v}_1 + \vec{v}_2 = \vec{v}_2 + \vec{v}_3 + \vec{v}_4 \\ &\text{B:} \quad \vec{v}_4 = \vec{v}_5 \\ &\text{C:} \quad \vec{v}_2 + \vec{v}_3 + \vec{v}_5 = \vec{v}_2 + \vec{v}_6 \end{aligned} \tag{1}$$

where $\vec{v}_2$, $\vec{v}_3$, $\vec{v}_4$ are the free fluxes and the remaining fluxes can be expressed as:

$$\begin{aligned} &\vec{v}_6 = \vec{v}_1 \\ &\vec{v}_5 = \vec{v}_4 \\ &\vec{v}_2 = \vec{v}_2 + \vec{v}_3 + \vec{v}_4 - \vec{v}_1 \end{aligned} \tag{2}$$

The balance equation for isotopomer distributions are derived as follows.

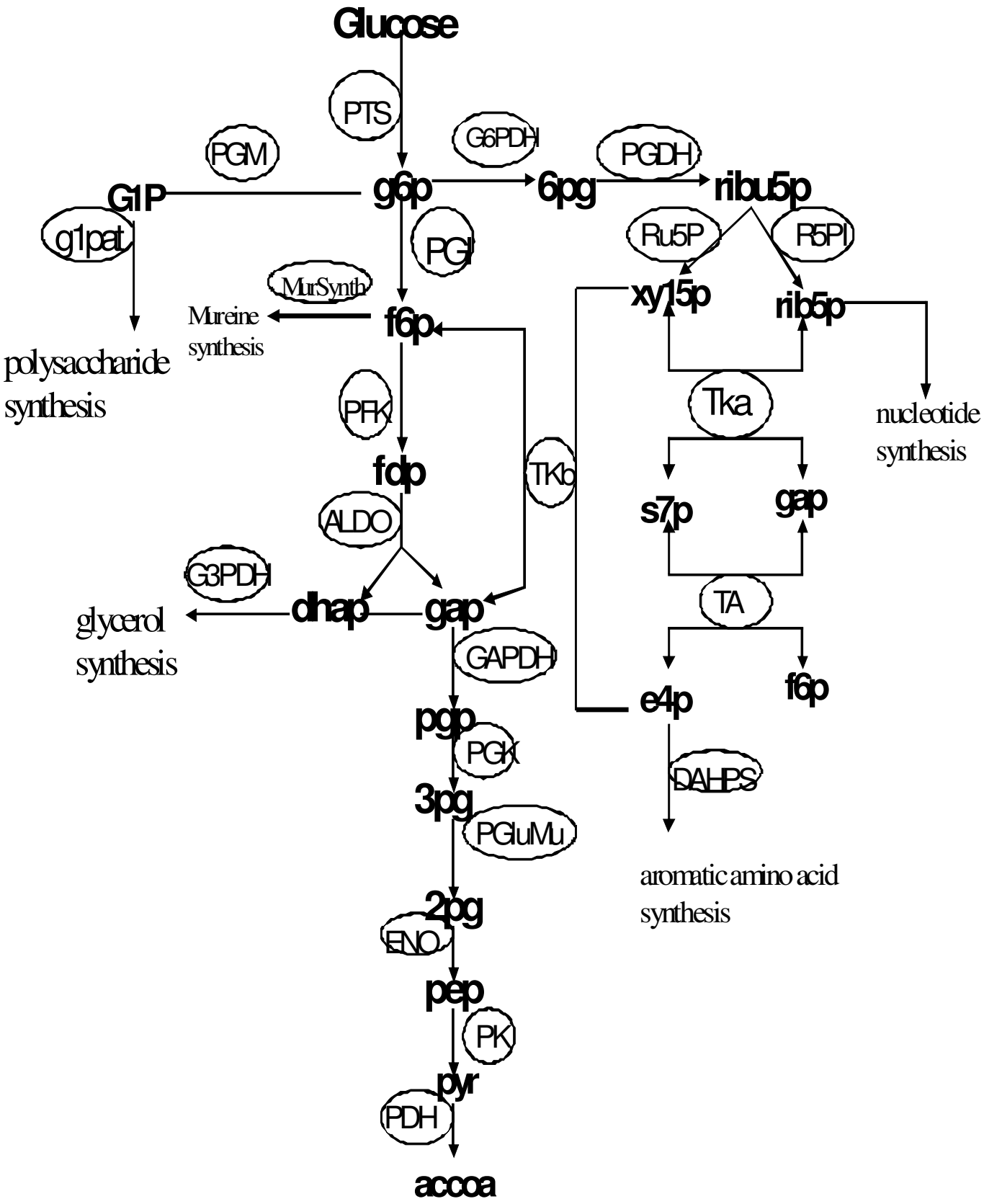

Figure 2. Metabolic network of *E. coli* central carbon metabolism of glycolysis and pentose phosphate (PP) pathway. Oval indicates the enzyme which catalyses the corresponding reaction. See text for the enzyme names.

$$A_{01}: (\vec{v}_2+\vec{v}_3+\vec{v})a_{01}=\vec{v}_2c_{01}+\vec{v}_1s_{01}$$

$$A_{10}: (\vec{v}_2+\vec{v}_3+\vec{v})a_{10}=\vec{v}_2c_{10}+\vec{v}_1s_{10}$$

$$A_{11}: (\vec{v}_2+\vec{v}_3+\vec{v})a_{11}=\vec{v}_2c_{11}+\vec{v}_1s_{11}$$

$$B_1: 2\vec{v}_5b_1=\vec{v}_4a_{01}+\vec{v}_4a_{10}+2\vec{v}_4a_{11}$$

$$C_{01}: (\vec{v}_2+\vec{v}_6)c_{01}=\vec{v}_2a_{01}+\vec{v}_3a_{10}+\vec{v}_5(1-b_1)b_1$$

$$C_{10}: (\vec{v}_2+\vec{v}_6)c_{01}=\vec{v}_2a_{10}+\vec{v}_3a_{01}+\vec{v}_5(1-b_1)b_1$$

$$C_{11}: (\vec{v}_2+\vec{v}_6)c_{11}=\vec{v}_2a_{11}+\vec{v}_3a_{11}+\vec{v}_5b^2{}_1 \quad (3)$$

where $a_{ij},\ b_i, c_{ij}, s_{ij}\ \ (i,j=0,1)$ are the isotopomer fractions of A, B, C and S, respectively. Since the sum of all isotopomer fractions of a metabolite must be 1, A_{00} B_{00} and C_{00} are computed by this relationship. The following relationships can be derived:

$$a_{01}+a_{10}+2a_{11}=2b_1=c_{01}+c_{10}+2c_{11}=s_{01}+s_{10}+2s_{11} \quad (4)$$

$$a_{01}-a_{10}=\vec{v}_1(\vec{v}_2+\vec{v}_3+\vec{v}_4)(s_{01}-s_{10})/d_1 \quad (5)$$

where,

$$d_1=\left(2\vec{v}_3{}^2+\vec{v}^2{}_4+2\vec{v}_2\vec{v}_3+\vec{v}_2\vec{v}_4+3\vec{v}_3\vec{v}_4+\vec{v}_1\vec{v}_2-\vec{v}_1\vec{v}_3\right)$$

$$a_{11}=\{4(\vec{v}_1\vec{v}_2+\vec{v}_1\vec{v}_3+\vec{v}_1\vec{v}_4)s_{11}+(\vec{v}_2\vec{v}_4+\vec{v}_3\vec{v}_4+\vec{v}_4^2-\vec{v}_1\vec{v}_4)(s_{01}+s_{10}+2s_{11})^2\}/d_2 \quad (6)$$

$$c_{11}=\left\{4\vec{v}_1(\vec{v}_2+\vec{v}_3)s_{11}+\vec{v}_4(\vec{v}_2+\vec{v}_3+\vec{v}_4)(s_{01}+s_{10}+2s_{11})^2\right\}/d_2 \quad (7)$$

where,

$$d_2=4\left\{(\vec{v}_2+\vec{v}_3+\vec{v}_4)^2-(\vec{v}_2+\vec{v}_3+\vec{v}_4-\vec{v}_1)(\vec{v}_2+\vec{v}_3)\right\}$$
$$=4\left(\vec{v}^2{}_4+\vec{v}_2\vec{v}_4+\vec{v}_3\vec{v}_4+\vec{v}_1\vec{v}_2+\vec{v}_1\vec{v}_3\right) \quad (8)$$

The mass isotopomer distributions of metabolites $A\left(m_0{}^a, m^a{}_1, m_2{}^a\right)$ etc. and the multiplet patterns of the second carbon of $A\left(S^a{}_{c2}, d^a{}_{c2}\right)$ etc. can be measured by 2D NMR. Thus the following relationships can be utilized.

$$a_{11}=m_2{}^a \quad c_{01}+c_{10}=m_1{}^c, \quad c_{11}=m_2{}^c$$

$$\frac{a_{01}}{a_{01}+a_{11}}=S_{c2}{}^a \text{ and } \frac{c_{01}}{c_{01}+c_{11}}=S_{c2}{}^a \quad (9)$$

From Equations (6) and (8), the values of $m^a{}_2$ and $m_2{}^c$ can be obtained respectively. Based on the above relationships we have the remaining parameters as follows:

$$a_{01}+a_{10}=s_{01}+s_{10}+2s_{11}-\{8\vec{v}_1(\vec{v}_2+\vec{v}_3+\vec{v}_4)s_{11}$$
$$+2\vec{v}_4(\vec{v}_2+\vec{v}_3+\vec{v}_4-\vec{v}_1)(s_{01}+s_{10}+s_{11})^2\}/d_2=m_1{}^a \quad (10)$$

$$c_{10}+c_{10}=m_1{}^c=s_{01}+s_{10}+2s_{11}-\left[8\vec{v}_1(\vec{v}_2+\vec{v}_3)s_{11}\right.$$
$$\left.+2\vec{v}_4(\vec{v}_2+\vec{v}_3+\vec{v}_4)(s_{01}+s_{10}+s_{11})^2\right]/d_2 \quad (11)$$

$$\frac{a_{01}}{a_{01}+a_{11}}=s_{c2}{}^a=1-$$
$$\frac{2d_1\left\{4(\vec{v}_1\vec{v}_2+\vec{v}_1\vec{v}_3+\vec{v}_1\vec{v}_4)s_{11}+(\vec{v}_2\vec{v}_4+\vec{v}_3\vec{v}_4+\vec{v}_4{}^2-\vec{v}_1\vec{v}_4)(s_{01}+s_{10}+2s_{11})^2\right\}_1}{d_2\{(\vec{v}_1\vec{v}_2+\vec{v}_1\vec{v}_3+\vec{v}_1\vec{v}_4)(s_{01}-s_{10})+d_1(s_{01}+s_{10}+2s_{11})\}} \quad (12)$$

and

$$\frac{c_{01}}{c_{10}+c_{11}}=s_{c2}{}^c=1-$$
$$-\frac{2d_1\left\{4(\vec{v}_1\vec{v}_2+\vec{v}_1\vec{v}_3)s_{11}+(\vec{v}_2\vec{v}_4+\vec{v}_3\vec{v}_4+\vec{v}^2{}_4)(s_{01}+s_{10}+2s_{11})^2\right\}}{\{(\vec{v}_1\vec{v}_2-\vec{v}_1\vec{v}_3)(s_{01}-s_{10})+d_1(s_{01}+s_{10}+2s_{11})\}d_2} \quad (13)$$

It should be noted that while it is possible to formulate both the net and exchange fluxes for bidirectional fluxes in a simple reaction network as given in the above example, it is usually not possible to derive the similar equation for large and complex metabolic system.

Model building and simulation

The approaches to modeling and simulation for the metabolic pathways include differential equations and metabolic control theory (Mendes, 1997). The fundamental entities to simulate are determined by the knowledge of biochemical system, generally at the level of metabolites and enzymes. And a model defined in terms of enzymes and reaction they catalyze, the rate of a reaction and the conditions under which a reaction proceeds is elucidated here at the present study. Differential equations have been widely used in the modeling and simulation of the metabolic pathways. The use of differential equations may work in case of complex and nonlinear systems (Raczynski, 1996). For the purpose of our study, we briefly describe the model equations developed by Chassagnole et al. (2002).

Phosphotransferase system (PTS)

The kinetic rate equation for the metabolic reaction Glc + PEP → G6P + PYR with enzyme PTS (Chassagnole et al., 2002) is expressed as,

$$r_{PTS}=\frac{r_{PTS}^{\max}C_{glc}^{extra}\frac{C_{pep}}{C_{pyr}}}{(K_{PTS,a1}+K_{PTS,a2}\frac{C_{pep}}{C_{pyr}}+K_{PTS,a3}C_{glc}^{extra}+C_{glc}^{extra}\frac{C_{pep}}{C_{pyr}})(1+\frac{C_{g6p}^{nPTS,g6p}}{K_{PTS,g6p}})} \quad (14)$$

Embden- Meyerhof-Parnas pathway

The kinetic rate equation for the metabolic reaction $G6P \Leftrightarrow F6P$ catalyzed by enzyme PGI (Phosphoglucosisomerase) which is reversible Michaelis-Menten kinetic type (Richter et al., 1975) is expressed as,

$$r_{PGI} = \frac{r_{PGI}^{\max}(C_{g6p} - \frac{C_{f6p}}{K_{PGI,eq}})}{K_{PGI,g6p}(1+\frac{C_{f6p}}{K_{PGI,f6p}(1+\frac{C_{6pg}}{K_{PGI,f6p,6pginh}})} + \frac{C_{6pg}}{K_{PGI,g6p,6pginh}}) + C_{g6p}}$$

(15)

For metabolic equation $F6P + ATP \Leftrightarrow FDP + ADP$ catalyzed by the enzyme PFK (phosphofructokinase) along with the allosteric type of enzyme reaction rate equation (Hofmann and Kopperschlager, 1982) may be expressed as,

$$r_{PFK} = \frac{r_{PFK}^{\max} C_{atp} C_{f6p}}{(C_{atp} + K_{PFK,atp,s}(1+\frac{C_{atp}}{K_{PFK,adp,c}}))(C_{f6p} + K_{PFK,f6p,s}\frac{A}{B})(1+\frac{L_{PFK}}{(1+C_{f6p}\frac{B}{K_{PFK,f6p,s}A})^{n_{PFK}}})}$$

(16)

$$A = 1 + \frac{C_{pep}}{K_{PFK,pep}} + \frac{C_{atp}}{K_{PFK,adp,b}} + \frac{C_{amp}}{K_{PFK,amp,b}}$$

$$B = 1 + \frac{C_{atp}}{K_{PFK,adp,a}} + \frac{C_{amp}}{K_{PFK,amp,a}}$$

For metabolic reaction $FDP <=> \mathrm{GAP} + \mathrm{DHAP}$ catalyzed by enzyme ALDO (Adolase) with the ordered uni-bi mechanism (Richter et al., 1975), the kinetic type rate equation is expressed as,

$$r_{ALDO} = \frac{r_{ALDO}^{MAX}(c_{FDP} - \frac{c_{GAP}c_{DHAP}}{K_{ALDO,eq}})}{K_{ALDO,fdp} + C_{fdp} + \frac{K_{ALDO,gap}C_{dhap}}{K_{ALDO,eq}V_{ALDO,b1f}} + \frac{K_{ALDO,dhap}C_{gap}}{K_{ALDO,eq}V_{ALDO,b1f}} + \frac{C_{fdp}C_{gap}}{K_{ALDO,gap,inh}} + \frac{C_{dhap}C_{gap}}{K_{ALDO,eq}V_{ALDO,b1f}}}$$

(17)

For the metabolic reaction $DHAP <=> \mathrm{GAP}$ catalyzed by enzyme TIS (triosephosphate isomerase) with the reversible Michaelis-Menten (Richter et al., 1975), the kinetic rate equation is given by:

$$r_{TIS} = \frac{r_{TIS}^{\max}(C_{dhap} - \frac{C_{gap}}{K_{TIS,eq}})}{K_{TIS,dhap}(1+\frac{C_{gap}}{K_{TIS,gap}}) + C_{dhap}}$$

(18)

For the reaction $ADP + PGP <=> 3\mathrm{PG} + \mathrm{ATP}$ catalyzed by the enzyme PGK (phosphoglycerate kinase) having the two substrate reversible Michaelis-Menten (Chassagnole, 2002) the kinetic rate equation is expressed as:

$$r_{PGK} = \frac{r_{PGK}^{\max}(C_{adp}C_{pgp} - \frac{C_{atp}C_{3pg}}{K_{PGK,eq}})}{(K_{PGK,adp}(1+\frac{C_{atp}}{K_{PGK,atp}}) + C_{adp})(K_{PGK,pgp}(1+\frac{C_{3pg}}{K_{PGK,3pg}}) + C_{pgp})}$$

(19)

For the metabolic reaction $GAP + NAD <=> \mathrm{PGP} + \mathrm{NADH}$ catalyzed by GAPDH (Glyceraldehyde 3-phosphate dehydrogenase) having the two-substrate reversible Michaelic-Menten (Chassagnole et al., 2002) the kinetic rate equation is expressed as,

$$r_{GAPDH} = \frac{r_{PGK}^{\max}(C_{gap}C_{nad} - \frac{C_{pgp}C_{nadh}}{K_{GAPDH,eq}})}{(K_{GAPDH,gap}(1+\frac{C_{pgp}}{K_{GAPDH,pgp}}) + C_{gap})(K_{GAPDH,nad}(1+\frac{C_{nadh}}{K_{GAPDH,nadh}}) + C_{nad})}$$

(20)

For the metabolic reactions $3PG <=> 2\mathrm{PG}$ and $2PG <=> PEP$ catalyzed by enzyme PGluMu (phosphoglycerate mutase) and ENO (enolase), respectively, having the reversible Michaelis-Menten (Chassagnole et al., 2002), the kinetic rate equations are respectively given by,

$$r_{PGluMu} = \frac{r_{PGluMu}^{\max}(C_{3pg} - \frac{C_{2pg}}{K_{PGluMu,eq}})}{K_{PGluMu,3pg}(1+\frac{C_{2pg}}{K_{PGluMu,2pg}}) + C_{3pg}}$$

(21)

$$r_{ENO} = \frac{r_{ENO}^{\max}(C_{2pg} - \frac{C_{pep}}{K_{ENO,eq}})}{K_{ENO,2pg}(1+\frac{C_{pep}}{K_{ENO,pep}}) + C_{2pg}}$$

(22)

For the equation $PEP + ADP <=> \mathrm{PYR} + \mathrm{ATP}$ catalyzed by PK (pyruvate kinase) with allosteric regulation, the kinetic rate equation (Johannes and Hess, 1973) is described as,

$$r_{PK} = \frac{r_{PK}^{\max} C_{pep}(\frac{C_{pep}}{K_{PK,pep}}+1)^{(n_{PK}-1)} C_{adp}}{K_{PK,pep}(L_{PK}(\frac{1+\frac{C_{atp}}{K_{PK,atp}}}{\frac{C_{fdp}}{K_{PK,fdp}}+\frac{C_{amp}}{K_{PK,amp}}+1})^{n_{PK}} + (\frac{C_{pep}}{K_{PK,pep}}+1)^{n_{PK}})(C_{adp} + K_{pk,adp})}$$

(23)

For the last equation of EMP pathway in *E. coli* $PYR <=> \mathrm{ACA} + \mathrm{CO_2}$ catalyzed by PDH (pyruvate dehydrogenase) along with the Hill equation (Chassagnole et al., 2002) the kinetic rate equation is given by,

$$r_{PDH} = \frac{r_{PDH}^{\max} C_{pyr}^{n_{PDH}}}{K_{PDH,pyr} + C_{pyr}^{n_{PDH}}}$$

(24)

Pentose-phosphate pathway (PPP): The first metabolic reaction $G6P + NADP <=> 6\mathrm{PG} + \mathrm{NADPH}$ of PP pathway in *E. coli* catalyzed by enzyme G6PHD (glucose-6-phosphate dehydrogenase) under the two-substrate irreversible Michaelis-Menten, the kinetic rate equation (Vaseghi et al., 1999) is given by,

$$r_{G6PDH} = \frac{r_{G6PDH}^{\max} C_{g6p} C_{nadp}}{(C_{g6p} + K_{G6PDH,g6p})(1 + \frac{C_{nadph}}{K_{G6PDH,nadph,g6pinh}})(K_{G6PDH,nadp}(1 + \frac{C_{nadph}}{K_{G6PDH,nadph,nadpinh}}) + C_{nadp})}$$

(25)

For the reaction $6PG + NADP <=> \mathrm{RiBu5P} + \mathrm{CO_2} + \mathrm{NADPH}$ catalyzed by PGDH (6-phosphogluconate dehydrogenase) under the two-substrate irreversible Michaelis-Menten kinetic rate equation (Vaseghi et al., 1999) the rate equation is given by,

$$r_{PGDH} = \frac{r_{PGDH}^{\max} C_{6pg} C_{nadp}}{(C_{6pg} + K_{PGDH,6pg})(C_{nadp} + K_{PGDH,nadp}(1 + \frac{C_{nadph}}{K_{PGDH,nadph,inh}})(1 + \frac{C_{atp}}{K_{PGDH,atp,inh}}))}$$

(26)

For metabolic reaction $RiBu5P <=> Rib5P$ catalyzed by R5PI (Ribose phosphate isomerase) under the reversible mass action kinetic type (Chassagnole et al., 2002), the rate equation is expressed as,

$$r_{R5PI} = r_{R5PI}^{\max} (C_{ribu5p} - \frac{C_{rib5p}}{K_{R5PI,eq}})$$

(27)

For metabolic reaction $RiBu5P <=> \mathrm{XY15P}$ catalyzed by Ru5p (ribulose phosphate epimerase) under the reversible mass action kinetic type (Chassagnole et al., 2002), the rate equation is expressed as,

$$r_{Ru5p} = r_{Ru5p}^{\max} (C_{ribu5p} - \frac{C_{xy15p}}{K_{Ru5p,eq}})$$

(28)

For metabolic reaction $Rib5P + XY15P <=> \mathrm{S7P} + \mathrm{GAP}$ catalyzed by Tka (transketolase a) under the reversible mass action kinetic type (Chassagnole et al., 2002), the rate equation is expressed as,

$$r_{TKa} = r_{TKa}^{\max} (C_{rib5p} C_{xy15p} - \frac{C_{s7p} C_{gap}}{K_{TKa,eq}})$$

(29)

For the metabolic reaction $S7P + GAP <=> \mathrm{F6P} + \mathrm{E4P}$ catalyzed by TA (Transketolase) under the reversible mass action kinetic type (Chassagnole et al., 2002) the rate equation is expressed as,

$$r_{TA} = r_{TA}^{\max} (C_{gap} C_{s7p} - \frac{C_{e4p} C_{f6p}}{K_{TA,eq}})$$

(30)

And for the metabolic reaction $XY15P + E4P <=> F6P + GAP$ catalyzed by the enzyme TKb (Transketolase b) under the reversible mass action kinetic type (Chassagnole et al., 2002) the rate equation is expressed as,

$$r_{TKb} = r_{TKb}^{\max} (C_{xy15p} C_{e4p} - \frac{C_{f6p} C_{gap}}{K_{TKb,eq}})$$

(31)

Analytic functions for cometabolites

$$C_{atp} = 4.27 - 4.163 \frac{t}{0.657 + 1.43t + 0.364t^2}$$

$$C_{adp} = 0.582 + 1.73\left(2.731^{-0.15t}\right)\left(0.12t + .000214t^3\right)$$

$$C_{amp} = 0.123 + 7.25\frac{t}{7.25 + 1.47t + 0.17t^2} + 1.073\frac{t}{1.29 + 8.05t}$$

$$C_{nadph} = 0.062 + 0.332\left(2.718^{-0.464t}\right)\left(0.016t^{1.58} + 0.00016t^{4.73} + 1.13_{10}^{-10}t^{7.89} + 1.36_{10}^{-13}t^{11.0} + 1.23_{10}^{-16}t^{14.2}\right)$$

$$C_{nadp} = 0.159 + 0.00554\frac{t}{2.8 + 0.271t + 0.01t^2} + 0.182\frac{t}{4.81 + 0.526t}$$

$$C_{nadh} = 0.0934 + 0.0011\left(2.371^{-0.123t}\right)\left(0.844t + 0.104t^3\right)$$

$$C_{nad} = 1.314 + 1.314\left(2.73^{(-0.0435t - 0.342)}\right) - \frac{(t + 7.871)\left(2.73^{(-0.0218t - 0.171)}\right)}{8.481 + t}$$

(32)

RESULTS AND DISCUSSIONS

Computer simulation was made using the mathematical model described above where the model parameter values are given in Chassagnole et al. (2002) and Rizzi et al. (1997). The MATLAB and GEPASI were used for simulation. Figures 3 to 5 show the simulation results. The abbreviations for compounds, reactions and enzymes used as usual and presented in the Appendix A and B are as per common usage.

The graphs in Figure 3 depict the concentrations of cometabolites with respect to time. These simulation results were performed using the Equation (32). It can be seen for Figure 3 that concentration of ATP and its effect sharply decreased from 0 to 1 s and then increased slowly reaching its steady state condition after 20 s. In the case of ADP, it shows the opposite trend as compared with ATP, which is reasonable from biochemistry point of view. The concentration of NAD decreased little slowly

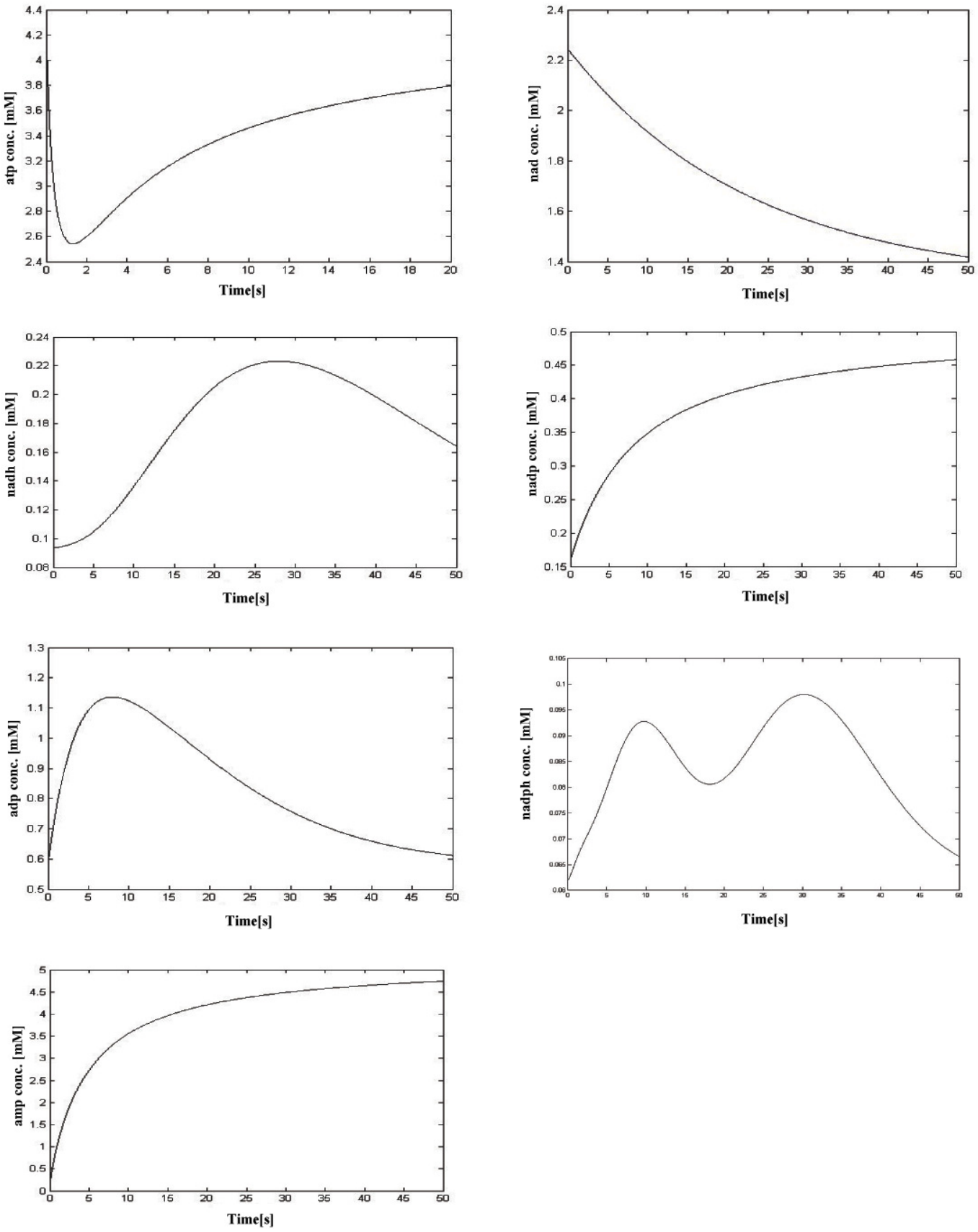

Figure 3. Simulation result for varying Concentrations of ATP, NAD, NADH, ADP, NADPH and AMP in *E.coli*.

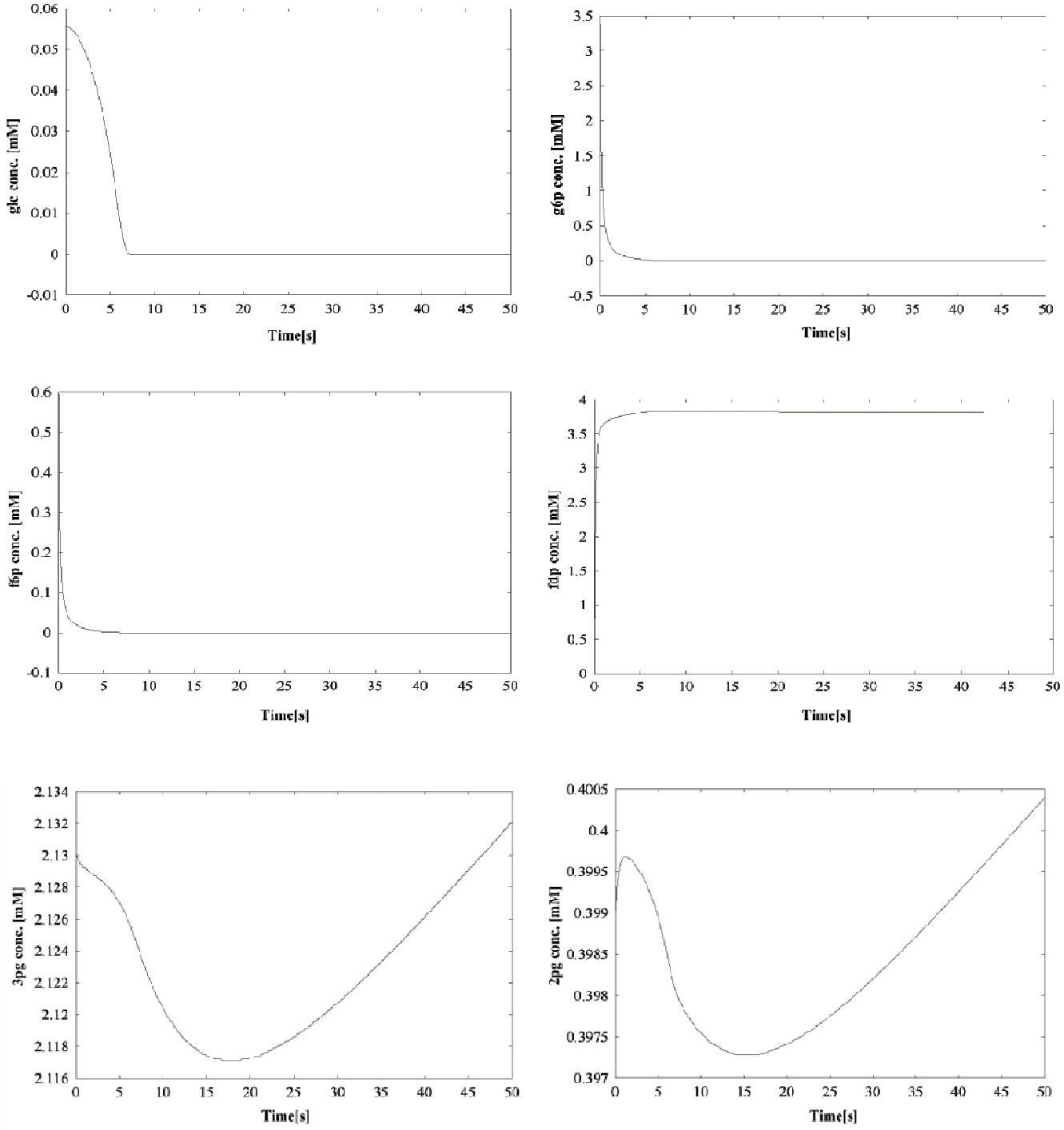

Figure 4. Time courses of the metabolite concentrations for Glc, G6P, F6P, FDP, 3PG, 2PG, PGP, DHAP, PEP, GAP, PYR, ATP, ADP, NAD and NADH in *E. coli*

until first 50 from its steady state. We also found from this figure that the concentration for NADH, NADP and AMP increased with few seconds where as concentration of NADPH increased first then oscillated to become its steady state.

The simulation results for the glycolysis and pp pathways are given in Figures 4 and 5, respectively. Figure 4 shows the concentrations of the metabolites Glc, G6P, F6P, FDP, 3PG, 2PG, PGP, DHAP, PEP, GAP, PYR, ATP, ADP, NAD and NADH with respect to time (s). The result shows that

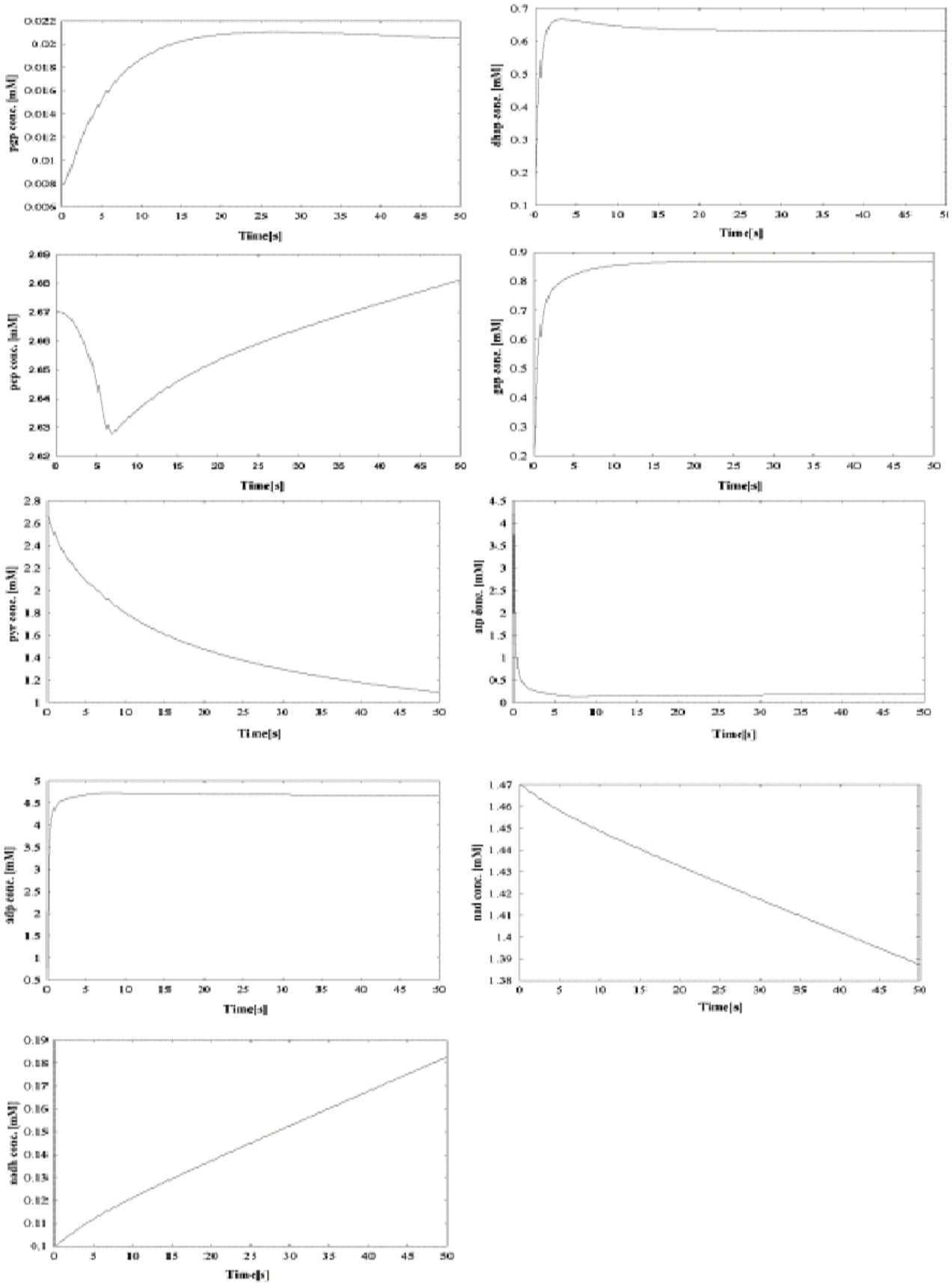

Figure 4. Continued…

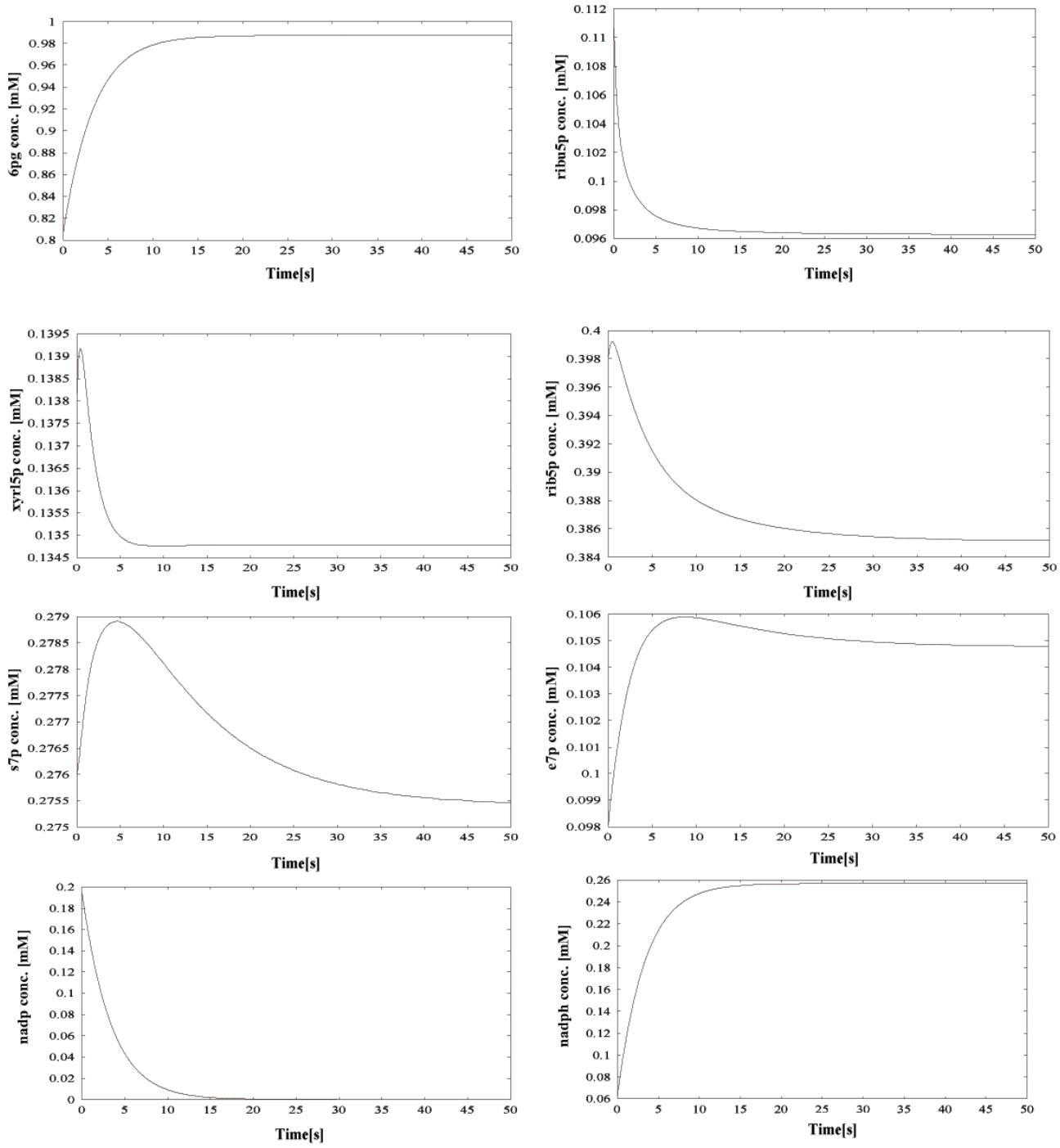

Figure 5. Time courses of the metabolite concentrations for 6PG, Ribu5P, XY15P, Rib5P, S7P, E4P, NADP and NADPH in *E. coli*

the concentration of Glc decreased sharply within 7 s from the start and then it became steady state at zero concentration and the PEP concentration sharply decreased and then increased again slowly reaching to its steady state after 50 s. The result shows the similar change in FDP, ADP and DHAP which are completely opposite results for concentration of ATP but almost the same results as was found for 3PG and 2PG and also the same results for GAP and PGP.

Figure 5 shows the concentrations of such metabolites as 6PG, Ribu5P, XY15P, Rib5P, S7P, E4P, NADP and NADPH with respect to time. The sharp increase in 6PG and nadph concentrations can be seen initially and then became steady state after a certain time. The opposite

trend can be seen for the concentrations of NADP, Ribu5P, Rib5P and XY15P. The concentrations of both S7P and E4P increased rapidly and then decreased sharply for S7P but slowly for E4P and finally became steady state after 40 and 30 s, respectively. These simulation results are mostly similar with published experimental results (Hoque et al., 2005). A stable steady state is an essential prerequisite for a mathematical model of living cells as well as for application of metabolic control analysis (Lui et al., 1996).

Conclusions

In the present study, we considered a simple model to understand basic idea on how to estimate the flux distribution based on measured data using NMR and GC-MS. Dynamic simulation of glycolysis and pentos-phosphate pathway in *E. coli* was made and validated with the initial concentrations using the kinetic rate equations for metabolites as well as using the analytic function for cometabolites. The simulation results give some idea on metabolic regulation, dynamic responses of intracellular metabolite concentrations and further analysis needs to be made. Although the intracellular metabolic fluxes can be analytically derived for the simple network considered in this study, more elaborate non-linear optimization techniques have to be considered for the more complex metabolic networks.

ACKNOWLEDGMENTS

This work was partly supported by a grant from the New Energy and Industrial Technology Development Organization (NEDO) of the Ministry of Economy, Trade and Industry of Japan. This study was also partially supported by a short research grant (PJP) of the University of Malaya, Malaysia. And partly funded by Japan Society for the Promotion of Science (JSPS).

REFERENCES

Chassagnole C, Rizzi NN, Schmid JW, Mauch K, Reuss M (2002). Dynamic modeling of the central carbon metabolism of *Escherichia coli.* Biotech. Bioeng. 79: 53-73.

Greco WR (1986). The role of simulation in biomedical modeling. Bulletin of mathematical biology. 48: 241-251.

He JH (2008). An allometric scaling law for understanding mammalian sleep. Afr. J. Biotechnol. 7(6): 712-713.

Hofmann E, Hopperschlager G (1982). Phosphosfructokinase in yeast. In: Wood WA, editor. Meth. Enzymol. New York: Academic Press. pp. 49-60.

Hoque MA, Ushiyama H, Tomita M, Shimizu K (2005). Dynamic responses of the intracellular metabolite concentrations of the wild type and pykA mutant *Escherichia coli* against pulse addition of glucose or NH_3 under those limiting continuous cultures. Biochem. Eng. J. 26 (1): 38-49.

Hua Q, Fu PC, Yang C, Shimizu K (1998). Microaerobic lysine fermentations and metabolic flux analysis. Biochem. Eng. J. 2: 89-100.

Johannes KJ, Hess B (1973). Allosteric kinetics of pyruvate kinase of *Saccharomyce cerevisiae*. J. Mol. Biol. 76: 181-205.

Lagunas R, Gancedo JM (1973). Reduced pyridine-nucleotides balance in glucose-growing *Saccharomyces cerevisae*. Eur. J. Biochem. 37: 90-94.

Lui J, Crawford JW, Viola R, (1996). The consequences of interactive noise for understanding the dynamics of complex biochemical systems. Dynam Stabil Syst. 11: 135-148.

Mendes P (1997). Biochemistry by numbers: Simulation of biochemical pathways with Gepasi 3. Trends in Biochemical Sci. 22 (9): 361-363.

Nogae I, Johnston M (1990). Isolation and characterization of the ZWF1 gene of *S. cerevisiae*, encoding glucose-6-phosphate dehydro-genase. Gene. 96: 161-169.

Noronha SB, Yeh HJC, Spande TF, Shiloach J (2000). Investigation of the TCA cycle and the glyoxylate shunt in *Escherichia coli* BL21 and JM109 using ^{13}C-NMR/MS. Biotechnol. Bioeng. 68: 316-327.

Park SM, Shaw RC, Sinskey AJ, Stephanopoulos G (1997). Elucidation of anaplerotic pathways in *Corynebacterium glutamicum* via ^{13}C - NMR spectroscopy and GC-MS. Appl. Microbiol. Biotechnol. 47: 430-440.

Raczynski S (1996). When System Dynamics ODE Models Fail. Simulation. 65(5): 343-349.

Richter O, Betz A, Giersch C (1975). The response of oscillating glycolysis in the NADH/NAD system: A comparison between experiment and a computer model. Biosystems. 7: 137-146.

Rizzi M, Baltes M, Theobald U, Reuss M (1997). *In vivo* analysis of metabolic dynamics in *Saccharomyces cerevisiae*. 2. Mathematical model. Biotechnol. Bioeng. 55: 592-608.

Sonntag K, Schwinde J de Graaf AA, Marx A, Eikmanns BJ, Wiechert W, Sahm H (1995). ^{13}CNMR studies of fluxes in the central metabolism of *Corynebacterium glutamicum* during growth and overproduction of amino acids in batch cultures. Appl. Microbiol. Biotechnol. 44: 489-495.

Sarkar D, Siddiquee KAZ, Arau´zo-Bravo MJ, Oba T, Shimizu K (2008). Effect of cra gene knockout together with *edd* and *iclR* genes knockout on the metabolism in *Escherichia coli,* Arch. Microbiol. 190: 559–571.

Theobald U, Milinger W, Baltes M, Rizzi M, Reuss M (1997). *In vivo* analysis of metabolic dynamics in *Saccharomyces cerevisiae*: I. Experimental observations, Biotechnol. Bioeng. 55: 305-316.

Thomas D, Cherest H, Surdin-Kerjan Y (1991). Identification of the structural gene for glucose-6-phosphate dehydrogenase in yeast. Inactivation leads to nutritional requierment for organic sulfur. EMBO J. 10: 547-553.

Vallino JJ, Stepphanopoulos G (1993). Metabolic flux distribution in *Corynebacterium glutamincum* during growth and lysine overproduction. Biotechnol. Bioeng. 41: 633-646.

Vaseghi S, Baumeister A, Rizzi M, Reuss M (1999). *In vivo* dynamics of the pentose phosphate pathway in *Saccharomyces cerevisiae*. Metab Eng 1: 128-140.

Wierchert W, Siefke C, de Graaf AA, Marx A (1997). Bidirectional reaction steps in metabolic networks: II. Flux estimation and statistical analysis. Biotechnol. Bioeng. 55: 118-135.

Yang C, Hua Q, Shimizu K, (2002). Quantitative analysis of intracellular metabolic fluxes using GC-MS and two-dimensional NMR spectroscopy. J. Biosci. Bioeng. 93 (1): 78-87.

Zhou GM, Jiang PK, Mo LF (2009). Bamboo: a Possible Approach to the Control of Global Warming. Int. J. Nonlinear Sci. Numerical Simulation. 10(4): 547-550.

Appendix A. Stoichiometric equations of *E. coli.*

Glycolysis Pathway:			
	Enzymes	**Genes**	**Reactions**
1.	Phosphotransferase system	*pts*	Glucose + PEP <-> G6P + PYR
2.	Phosphoglucose isomerase	*pgi*	G6P <-> F6P
3.	Phosphofructokinase	*pfk*	F6P <-> GAP
4.	Phosphoglycerate kinase	*pgk*	GAP -> PEP + NADH + ATP
5.	Pyruvate kinase	*pyk*	PEP -> PYR + ATP
6.	Pyruvate dehydrogenase	*pdh*	PYR -> AcCoA + NADH + ATP
TCA Pathway:			
	Enzymes	**Genes**	**Reactions**
7.	Acetate kinase	*ack*	AcCoA -> Acetate + ATP
8.	Citrate synthase	*glt*	AcCoA + OAA -> ICT
9.	Isocitrate dehydrogenase	*icd*	ICT -> KG + NADH + CO_2
10.	Glyoxylate bypass (lumped reaction)	*ace*	AcCoA + ICT -> 2OAA + NADH
11.	2-ketoglutarate dehydrogenase	*AKGDH*	KG -> SUC + NADH + ATP +CO_2
12.	Malate dehydrogenase	*mdh*	SUC -> OAA + NADH + ATP
13.	PEP carboxylase	*ppc*	PEP +CO_2 -> OAA
PP Pathway:			
	Enzymes	**Genes**	**Reactions**
14.	Glucose-6-phosphate dehydrogenase	*zwf*	6PG -> RU5P + 2NADH + CO_2
15.	Ribose-5-phosphate isomerase	*rpi*	RU5P □> R5P
16.	Ribulose-5-phosphate epimerase	*rpe*	RU5P <-> XY5P
17.	Transketolase	*tkt*	R5P + X5P <-> GAP + S7P
18.	Transaldolase	*tal*	GAP + S7P <-> F6P +E4P
Two more reactions:			
		Genes	**Reactions**
19.	ATP degradation	J_{atp}	ATP ->
20.	Nad(p)h oxidation	J_{resp}	NAD(P)H -> 2ATP
Biomass Equation:			
205G6P+70.9F6P+1625GAP+519.1PEP+2832.8PYR+4028.8AcCoA+1786.7OAA+1078.9KG+ 897.7R5P+361E4P+14678NAD(P)H+18485ATP-> Cellmass + 1793CO_2 + 387Acetate			

Appendix B. Nomenclature.

Enzymes	
6PGDH	6-phosphogluconate dehydrogenase
Eno	enolase
Fba	fructose-1, 6-bisphosphate aldolase
G6PDH	glucose-6-phosphate dehydrogenase
GAPDH	glyceraldehydes-3-phosphate dehydrogenase
GDH	glutamate dehydrogenase
Hxk	hexokinase
ICDH	isocytrate dehydrogenase
LDH	lactate dehydrogenase
MDH	malate dehydrogenase
Mk	myokinase
Pgi	phosphoglucose isomerase
Ppc	phosphoenolpyruvate carboxylase
Pta	phosphotransacetylase
PTS	phosphotransferase system
Pyk	pyruvate kinase
Rpe	ribulose-phosphate epimerase
Rpi	ribose-phosphate isomerase
Tkt	transketolase
Tpi	Triosephosphate isomerase

Metabolites	
2PG	2-phosphoglycerate
6PG	6-phosphogluconate
AcCoA	acetyle-coenzyme A
ADP	adenosindinophosphate
AKG	α-ketoglutarate
AMP	adenosinmonophosphate
ATP	adenosintriphosphate
DHAP	dihydroxyacetonephosphate
E4P	erythrose-4-phosphate
F6P	fructose-6-phosphate
FBP	fructose-1,6-bisphosphate
G6P	glucose-6-phosphate
GAP	glyceraldehydes-3-phosphate
ICT	isocitrate
NAD	diphosphopyridindinucleotide, oxidized
NADH	diphosphopyridindinucleotide, reduced
NADP	diphosphopyridindinucleotide-phosphate, oxidized
NADPH	diphosphopyridindinucleotide-phosphate, reduced
OAA	oxaloacetate
PEP	phosphoenolpyruvate
PYR	pyruvate
Rib5P	ribose-5-phosphate
Ribu5p	ribulose-5-phosphate
SUC	succinate